Doxorubicin-Loaded Microrobots for targeted drug delivery and anticancer therapy

Sudipta Mallick[1], Ramadan Abouomar[1], David Rivas[1], Max Sokolich[1],

Fatma Ceren Kirmizitas[1,2], Aditya Dutta[2], and Sambeeta Das[1*]

[1]Department of Mechanical Engineering, University of Delaware,

[2]Department of Animal and Food Sciences, University of Delaware

[*]**Corresponding Author: samdas@udel.edu**

Abstract

Micro-sized magnetic particles (also known as Microrobots (MRs)) have recently been shown to have potential applications for numerous biomedical applications like drug delivery, microengineering, and single cell manipulation. Interdisciplinary studies have demonstrated the ability of these tiny particles to actuate under the action of a controlled magnetic field which not only drive MRs in a desired trajectory but also precisely deliver therapeutic payload to the target site. Additionally, optimal concentrations of therapeutic molecules can also be delivered to the desired site which is cost-effective and safe especially in scenarios where drug dose-related side effects are a concern. In this study, MRs were used to deliver anticancer drugs (doxorubicin) to cancer cells and subsequent cell death was evaluated in different cell lines (liver, prostate, and ovarian cancer cells). Cytocompatibility studies showed that MRs were well-tolerated and internalized by cancer cells. Doxorubicin (DOX) was chemically conjugated with MRs (DOX-MRs) and magnetically steered towards cancer cells using our magnetic controller. Time-lapsed video showed that cells shrunk and eventually died when MRs were internalized by cells. Taken together, this study confirms that microrobots are promising couriers for targeted delivery of therapeutic biomolecules for cancer therapy and other non-invasive procedures which require precise control.

Keywords: Microrobots, Doxorubicin, Cancer therapy, Drug delivery, Liver, Prostate, Ovary.

Introduction

Over the past couple of decades, there has been tremendous advancement in cancer therapy, with two distinct approaches – conventional and emerging therapies.[1-2] While conventional treatment methods include surgery followed by chemotherapy or radiation therapy, emerging categories include nanomedicine, immunotherapy (dendritic cell-based, antibody-based), and stem cell therapy.[2] To maximize efficacy, a combination of these therapies is also extensively practiced while avoiding serious side-effects.[3] Although significant progress has been achieved in the development of anticancer therapies and post-treatment management of cancer; delivering optimal therapeutic concentrations of anticancer agents to target sites without compromising quality of life is almost impossible with current standard of care.[4] More recently, cross-disciplinary approaches have helped revolutionized the way medical and health-care teams approach different health conditions.[5] The development of smart micro- and nano-swimmers that can self-actuate and navigate through complex biological systems have great potential to overcome various challenges in drug targeting and delivery.[6-8] Particularly, micro-sized robots (microrobots; MRs) are highly desirable because of their larger size compared to nano-robots, which allows them to be visualized under a microscope. The self-propulsion of MRs can be attained by various chemical/biochemical (such as H_2O_2, H_2O, and $NaBH_4$) and external energy fields (magnetic field, ultraviolet (UV), ultrasound). In recent years, MRs have been actively investigated for anticancer drug loading, delivery, and release.[9-10] Drugs have been incorporated onto MRs through physical adsorption, electrostatic interaction, and covalent linkage. Different structures such as spherical, rod-shaped, and helical MRs have been optimized to maximize drug-loading and propulsion efficiency. Several groups have reported helical MRs for Doxorubicin (DOX) delivery, and release by ultraviolet or near-infrared laser light irradiation.[11-14] These studies have used electromagnetic actuation mechanisms for targeting and light-triggered DOX release. Sun *et al.* has reported pine pollen-based MRs with two hollow sacs for magnetic particles, and DOX encapsulation.[15] Incorporation of magnetic particles allowed MRs to be propelled in different environments using three different motions (rolling, tumbling, and spinning). Another study has reported tri-magnetic bead MRs prepared by surface-functionalized biotin-streptavidin interaction for anticancer therapy.[16] Villa *et al.* has reported the use of superparamagnetic microrobots for drug delivery, and single cell manipulation.[17] Platinum-coated MRs were fabricated and driven in the presence of hydrogen peroxide (H_2O_2) where the speed of MRs was H_2O_2 concentration dependent, and above a safe limit. Moreover, platinum-coated MRs form chain-like structures in the presence of a magnetic field, and may interfere with the self-propulsion of MRs, and cellular uptake due to their bigger size. Currently magnetic microrobots involve complex fabrication processes, surface functionalization, complex propulsion techniques, and difficult to setup experiments with the magnetic field controller.

Moreover, biocompatibility of these microrobots is a big concern when drug delivery or other in vivo applications are involved. In addition, chemical and light driven (NIR laser) propulsion mechanisms for the microrobots involve toxic fuels or photoactive materials, and the stability of conjugated drug in such environments is dubious.[18] Furthermore, drug loading strategies via physical adsorptions (hydrogen bonding, Van der Waals bonding, electrostatic etc.) are either vulnerable to premature release or cause inadequate drug release.[18] Therefore, a microrobotic-based drug delivery system with simple fabrication process, easy to use magnetic controller, chemical drug loading and release mechanism while having adequate cancer killing ability without any external stimuli is desired.

In this study, we design a simple, yet effective strategy to prepare DOX-loaded MRs (DOX-MRs) that are self-propelled in presence of an external magnetic field. These microrobots are carboxylic group-functionalized paramagnetic beads which allow covalent conjugation of DOX on its outer surface (Fig. 1). These microrobots can be steered to any desired direction, and navigate through narrow, and confined space with precise control. Microrobots are ingested by cancer cells after DOX-MRs treatment, where DOX is cleaved, and released by proteolytic enzyme activity.

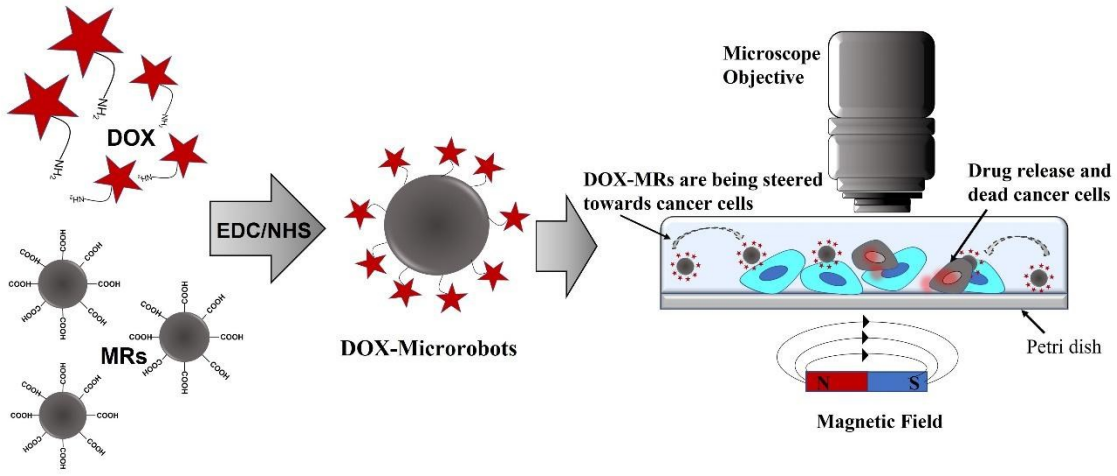

Figure-1: Schematic representation of Doxorubicin-conjugated Microrobots (DOX-MRs) and cancer cell death induced by magnetically steered DOX-MRs. DOX-MRs were driven in the horizontal plane using a wireless joystick. The strength and direction of the magnetic fields were controlled using a custom Matlab code. Real-time tracking of DOX-MRs and live cells were possible with our 3D printed petri dish-fitted microscope stage and set-up.

Materials and Methods

Paramagnetic beads (diameter- 4.7μm) were purchased from Spherotech (Cat. No. FCM-4056-2). Detailed characterization of beads (SEM, magnetization curve, functional group etc.) can be found on Spherotech website. Doxorubicin HCL was purchased from Sigma-Aldrich (Cat. No. 0000133488).

Preparation of DOX-MRs:

Doxorubicin was covalently conjugated to magnetic beads by ethyl (dimethylamino propyl) carbodiimide (EDC), and N-hydroxysuccinimide (NHS) coupling as described previously.[21]10 mg of magnetic beads was ultrasonically dispersed in 2 mL MilliQ water with 5-times excess EDC and NHS stirred for 2 hours. Doxorubicin (DOX concentration = 1 mg/mL) was added dropwise to the above solution, and stirred for 4 hours at room temperature, protected from light. DOX-MRs were collected using centrifugation at 12,000 RPM 30 min, 24 °C (Eppendorf centrifuge 5415 D). The supernatant was collected separately, while solid DOX-MR were washed with MilliQ water (2 mL × 3 times) until supernatant became clear, indicating the absence of free DOX in the sample. UV was then employed to quantify the amount of free/unloaded DOX molecules in the combined supernatants. From the free DOX determined by UV, loaded DOX can be quantified based on the initial amount of DOX in the original solution. A calibration curve was obtained from a serial dilution of stock solution containing pure DOX in MilliQ water (concentration 1 mg/mL).

Magnetic controller set up of microrobots:

Experiments were conducted on an Axioplan 2 upright microscope using an Axiovert 503 mono camera, and an Axiovert 200 inverted microscope with a Amscope MU903-65 camera. Experiments on the Axioplan microscope utilized a custom-built magnetic control system which applied magnetic field strengths at the sample from 3-7 mT. The magnetic coil configuration is a traditional four coil system and controlled via a custom python graphical user interface as outlined in [20]. The strength, and direction of the fields are controlled using custom python code. Experiments performed on the Axiovert microscope utilize hand-held permanent cylindrical magnets that produce magnetic field strengths at the sample of approximately 10-30 mT. The hand-held permanent magnets are used when translating the cells due to their ability to be placed in closer proximity to the cells and, therefore, allowing for stronger magnetic field gradients to be applied compared to the electromagnets. Paramagnetic beads used in the experiments were fluorescent, and had a diameter of 4.7 μm. The fluorescent microspheres were illuminated using an X-cite mini plus from Excelitas Technologies.

Cell culture:

Hepatocellular Carcinoma cells (HepG2), Prostate cancer cells (LNCaP cells), and Ovarian cancer cells (Caov-3 cells) were kindly gifted by Late Richard West (Associate Scientist at Flow Cytometry Core Facility), and our collaborators. Cells were cultured in Dulbecco's Modified Essential Medium (DMEM, Gibco, BenchStable, USA) media with 5% CO_2, and maintained at 37 °C in an incubator. All experiments were performed after second passage, and by eighth passage.

Assessment of Cytocompatibility of microrobots in normal cells:

Microrobots with different surface functionalities were evaluated in Human Embryonic Kidney cells (HEK-293) to evaluate cytocompatibility of microrobots in normal cells. Different MRs with different functional groups (primary amine, carboxylic, and neutral) were treated for 24 hours, and cellular internalization, and cytotoxicity were evaluated using flowcytometry.

Assessment of Cellular uptake of Microrobots in cancer cells:

Carboxylic group was chosen for DOX conjugation due to their comparable compatibility, and cellular uptake with neutral MRs. Therefore, carboxylic MRs were evaluated in all three cancer cell lines (HepG2, LNCaP, and Caov-3 cells). Cells were seeded (10^4 cells/well) in a clear 35 mm confocal dish (SPL, USA), and incubated in DMEM media with 5% CO_2 at 37 °C for 24 hours. Then, cells were treated with MRs (4.7 μM size, 1 mg/mL), and incubated for 24 hours. Cells were then imaged under optical microscope to check cell morphology. Cellular uptake of MRs was assessed as aforementioned method. Flow cytometry was performed to quantify cellular uptake of MRs in all cells. $1x10^6$ cells/well were seeded in a 6-well plate and incubated in DMEM with 5% CO_2 at 37 °C for 24 hours. Then, 20 μL of 1% w/v MRs (Carboxyfluorescein (green), 4.7 μM size) solution was added to the each well containing 2 mL media. After 24 hours, cells were washed, and analyzed using a flow cytometer (BD FACS Aria III).

Movement of MRs under the influence of Magnetic field:

Controlled movement and targeting ability of microrobots were assessed using our custom-built magnetic controller. Caov-3 cells were cultured ($5x10^5$ cells/mL) in a 35 mm petri dish at 37 °C with 5% CO_2. After 24 hours, MRs were added to the petri dish, and steered towards the cells using a wireless joystick. Images and videos were taken using an Axioplan 2 upright microscope using an Axiovert 503 mono camera, and an Axiovert 200 inverted microscope with a Amscope MU903-65 camera.

Characterization of DOX-MRs:

Dry samples were used to perform Scanning Electron Microscopy (SEM) to confirm morphology of

magnetic MRs after DOX conjugation. Fluorescence images of the same DOX-MRs samples were taken using a fluorescence microscope (Carl Zeiss Axiovert S100).

Anticancer effect of DOX-MRs:

HepG2, LNCaP, and Caov-3 cells were cultured ($1x10^5$ cells) in a 35 mm petri dish at 37 °C with 5% CO_2. After 24 hours, DOX-MRs were added to the petri dish, and incubated for 24 hours. Cell death was assessed using a confocal microscope. Another petri dish was imaged for time-lapse video of DOX-MR uptake, and cell death using a confocal microscope immediately after MRs addition.

Result and Discussion

Cyto-compatibility of Microrobots:

Biocompatibility is one of the most important factors while designing microrobots. In addition to being non-toxic, microrobots should not release any chemicals or by-products that is going to affect results during experiments. To assess the cytocompatibility, and cellular uptake, microrobots with different surface functional groups were investigated in HEK-293 cells. Neutral MRs showed highest cellular uptake as compared to carboxylic, and amine functionalized groups in HEK-293 cells. The mechanism of cellular uptake is presumably phagocytosis which includes two steps; adhesion followed by internalization. Polystyrene beads tend to adhere to the cell membrane, followed by internalization, and this adhesion step is affected by anionic or cationic charges of the beads.[19] Therefore, neutral MRs showed highest cellular uptake compared to other two charged MRs (Fig. 2, table). While neutral, and carboxylic MRs were nontoxic, amine MRs showed slightly toxic effect with 17% cell death (Fig. 2). Interestingly, multiple MRs were observed inside the cells showing high affinity of these polystyrene beads towards the cells.

Types of MRs	Size(µm)	Charge(mV)	Cellular uptake (%)
Carboxyl	4.7	-79.9	35.4
No functional group	4.35	-53.9	45
Primary amine	4.7	-28.1	32.2

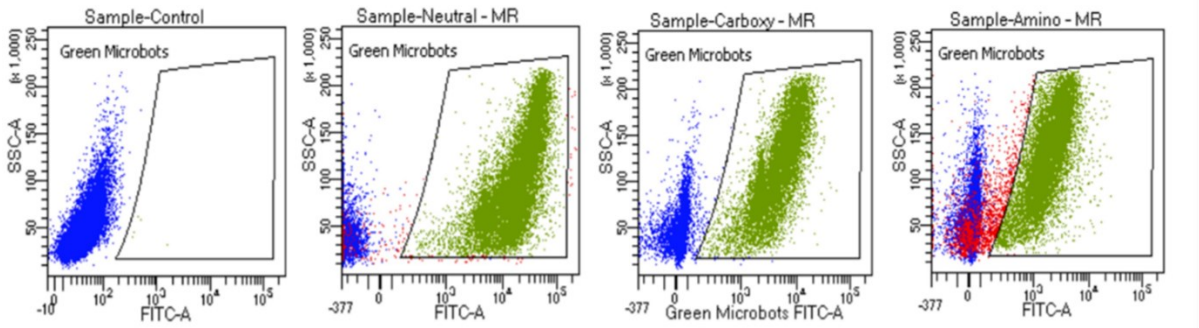

Cells with MRs - **0%**

Cells with MRs - **45%**
Dead cells - **1.3%**

Cells with MRs - **35.4%**
Dead cells - **0.3%**

Cells with MRs - **32.2%**
Dead cells - **8.7%**

Figure-2: Cytocompatibility study of MRs. (a) Table showing physiochemical characteristics of MRs with different functional groups and (b) representative flow cytometry data showing negligible percentage of cell death when incubated with MRs. Cell death was observed in case of primary amine-functionalized MRs due to their cationic nature, which was not significant. Cellular uptake was highest for neutral MRs compared to carboxylic- and primary amine-functionalized MRs.

Considering cytocompatibility, cellular uptake, and functional group for further DOX conjugation, carboxylic-MRs were selected for further experiments. Then, cytotoxicity of carboxylic-MRs was investigated in cancer cells such as HepG2, LNCaP, and Caov-3 cells. After 24 hours, changes in cell morphology were monitored using a confocal microscope. After 24 hours, cell morphology was found to be normal when compared with untreated control groups (Fig. 3a). To confirm that MRs are non-toxic, cells with MRs were sorted, and cultured for 24 hours. Cells were healthy with intact morphology (data not shown). However, we observed cells with multiple MRs (≥ 5) were eventually dead presumably due to interrupted cellular activity. This data confirmed that the magnetic MRs were suitable for biological applications.

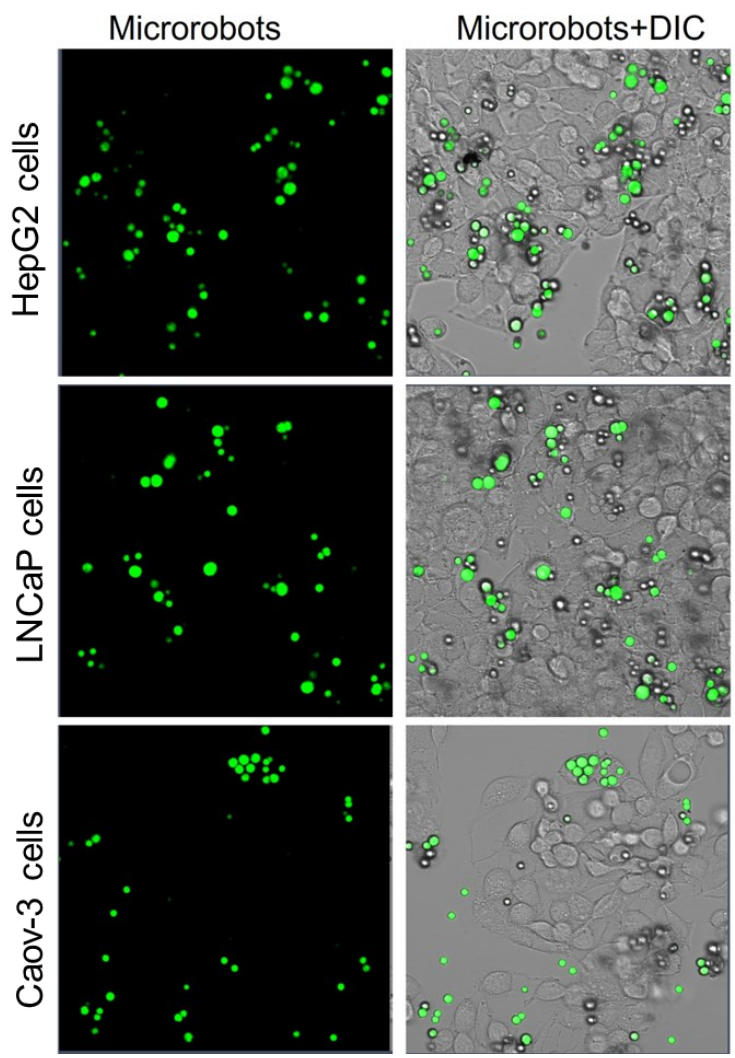
Microrobots
Microrobots+DIC
HepG2 cells
LNCaP cells
Caov-3 cells

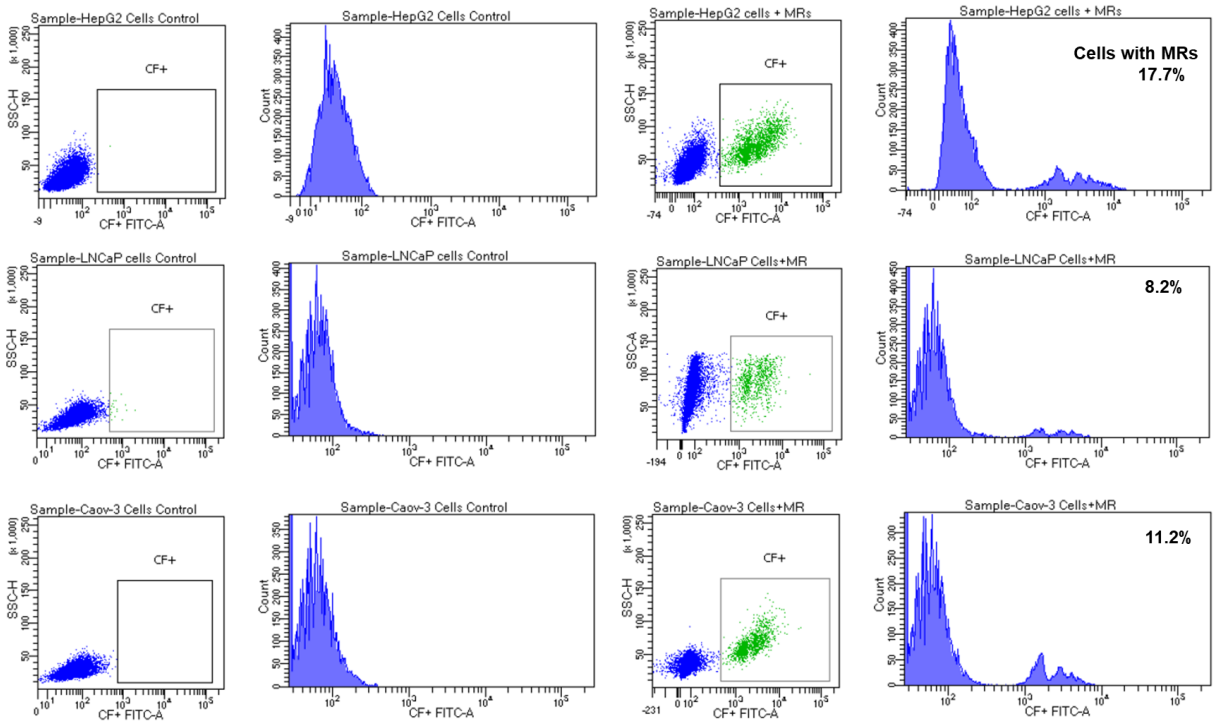

Figure-3: A comparative cytocompatibility (upper panel) and cellular uptake (lower panel) study of carboxylic group-MRs in three different cancer cell lines. Cell morphology was intact after 24 hours of incubation and cellular uptake of MRs was enhanced in HepG2 cells compared to LNCaP and Caov-3 cells.

Cell-internalization of Microrobots:

Cellular uptake is a crucial step to consider when cytotoxic drugs or drug delivery systems are developed or designed. Although carboxylic-MRs were cyto-compatible, cellular uptake in different cancer cells may vary depending on the complexity of different cancers. The cellular uptake results showed varying cellular uptake for three different cancer cells (Fig. 3b). HepG2 cells showed highest cellular uptake compared to ovarian and prostate cancer cell lines. This result can be better explained by considering the detoxification role of liver, and hepatocytes where ingestion of extracellular materials (here MRs) is inevitable.[22] Moreover, polystyrene beads may have different affinity towards different cancer cells.

Transport of MRs and cancer cell-targeting:

Experiments were carried out using our magnetic system described in Fig. 1. Paramagnetic magnetic MRs were transported from one assigned place to another, both on a plain surface, and cell grown petri dish using our custom-built magnetic controller. Helmholtz coils were used to generate a rotating magnetic

field that allows these MRs to roll along the surface of the substrate (Video-1). Experiments were carried out under a magnetic field strength of approximately 5 mT. Microrobots and HepG2 cells were aligned under our magnetic controller with a wireless joystick. Direction and strength of the magnetic field was controlled by custom Matlab code. Microrobots were steered to bring them closer to the cells (Fig. 4). Besides that, MRs were also able to roll over or by-pass cells due to the precision in our magnetic set up.

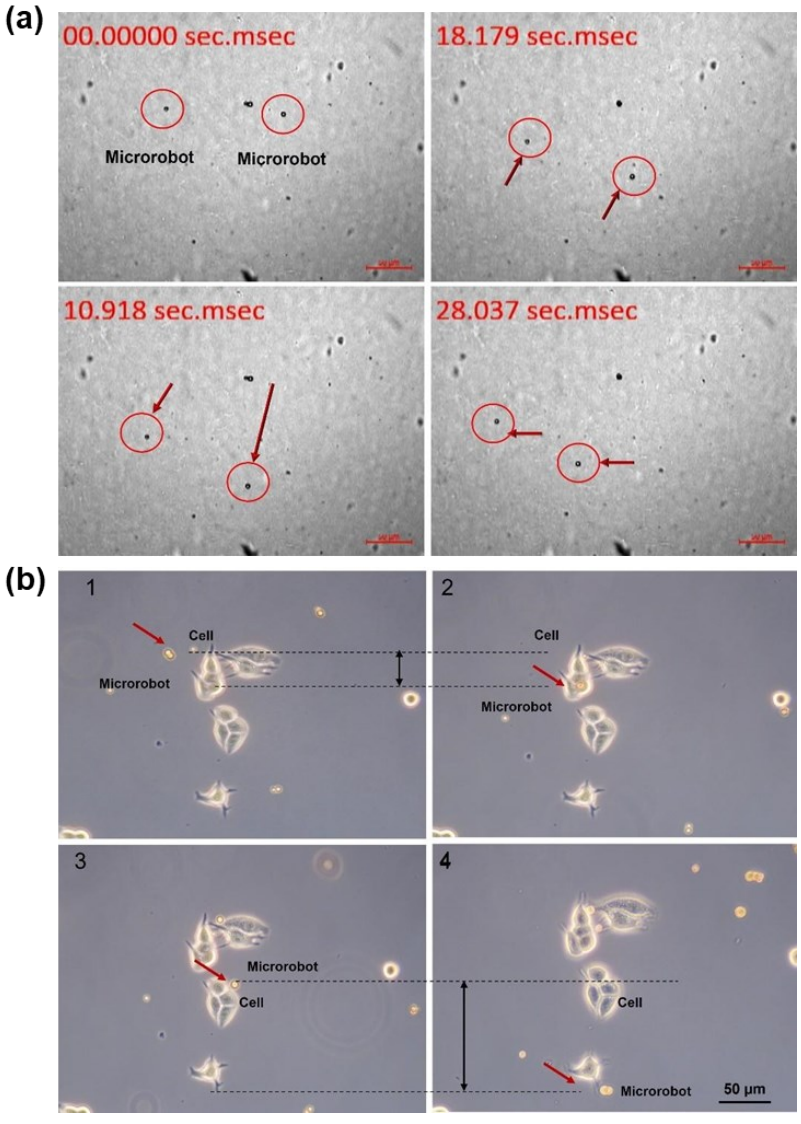

Figure-4: Microscopic images of MRs being driven to (a) any direction on the plane surface and (b) towards the cells using our magnetic controller. Direction of MRs was controlled using a wireless joystick.

Characterization of DOX-MRs:

The structural properties of MRs were confirmed by scanning electron microscope (SEM). Chemical conjugation of DOX with microrobots was also confirmed by fluorescence microscopy. As shown in Fig. 5, MRs are spherical in shape (size approximately, 5 μM) with rough surface (Fig. 5a). After coating, there were visible differences in roughness of the surface with increase in size of the microrobots confirming successful conjugation of DOX (Fig. 5b). Apart from that, intrinsic fluorescence of DOX was also used to confirm covalent linkage of DOX to MRs. Microrobots were imaged under a confocal microscope, and bright red fluorescence from beads confirmed successful conjugation of DOX on the surface of microrobots (Fig. 5c and d). We also checked the zeta potential of MRs after DOX-conjugation. The positive surface charge (+73mV) confirmed the presence of DOX loading on the surface of the MRs. While the maximum attachment capacity of DOX to these beads is 10μeq/g (equal to the manufacturer's claim of 10 μeq/g carboxyl groups), we believe all microrobots have an equal number of DOX molecules since excess amounts were added during conjugation experiments.

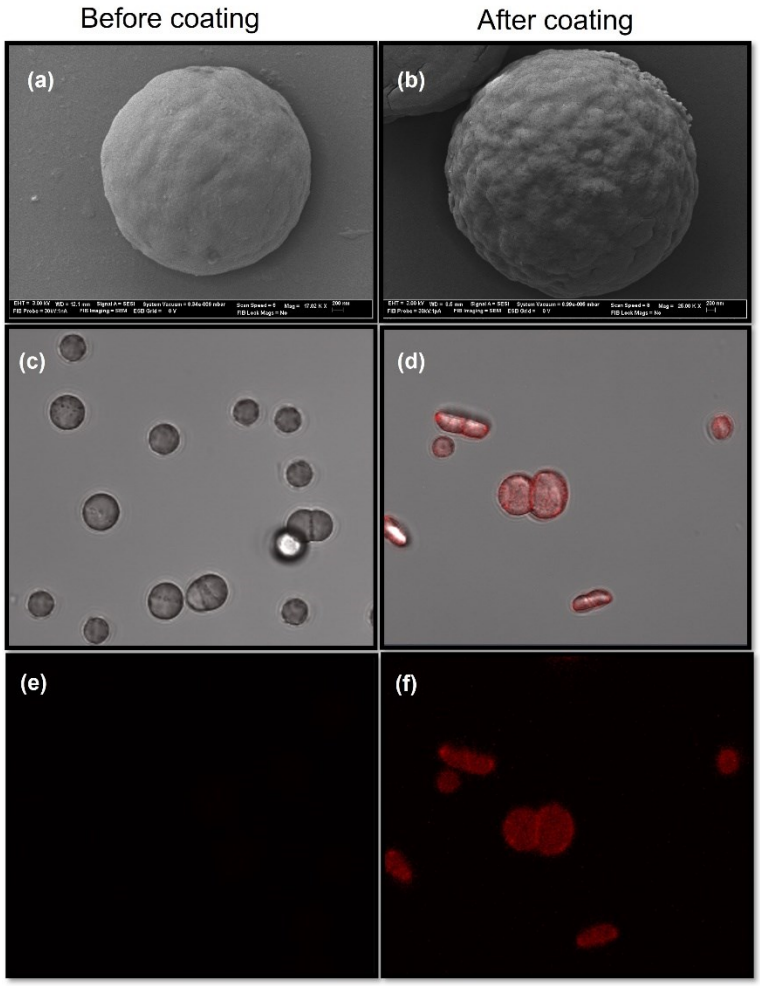

Figure-5: SEM images of microrobots (a) before and (b) after DOX coating. MR sizes were increased approximately 1µm after DOX coating which confirmed coating. Fluorescence images (c) before and (d) after-coating showed red fluorescence from MRs confirming successful conjugation of DOX on the surface of MRs.

Anticancer effect of DOX-MRs:

Doxorubicin is an anthracycline which is known to damage DNA or interfere in DNA replication that eventually leads to cell death. However, cytotoxic concentration of DOX must be delivered to kill cells. HepG2, LNCaP, and Caov-3 cells were treated with DOX-MRs, and DOX-induced cell death was assessed after 24 hours. Fluorescence images showed dead cells floating in the media with multiple MRs (Fig. 6). This indicates that cell death was DOX concentration dependent, and multiple MRs were able to deliver cytotoxic concentration of DOX to the cells.

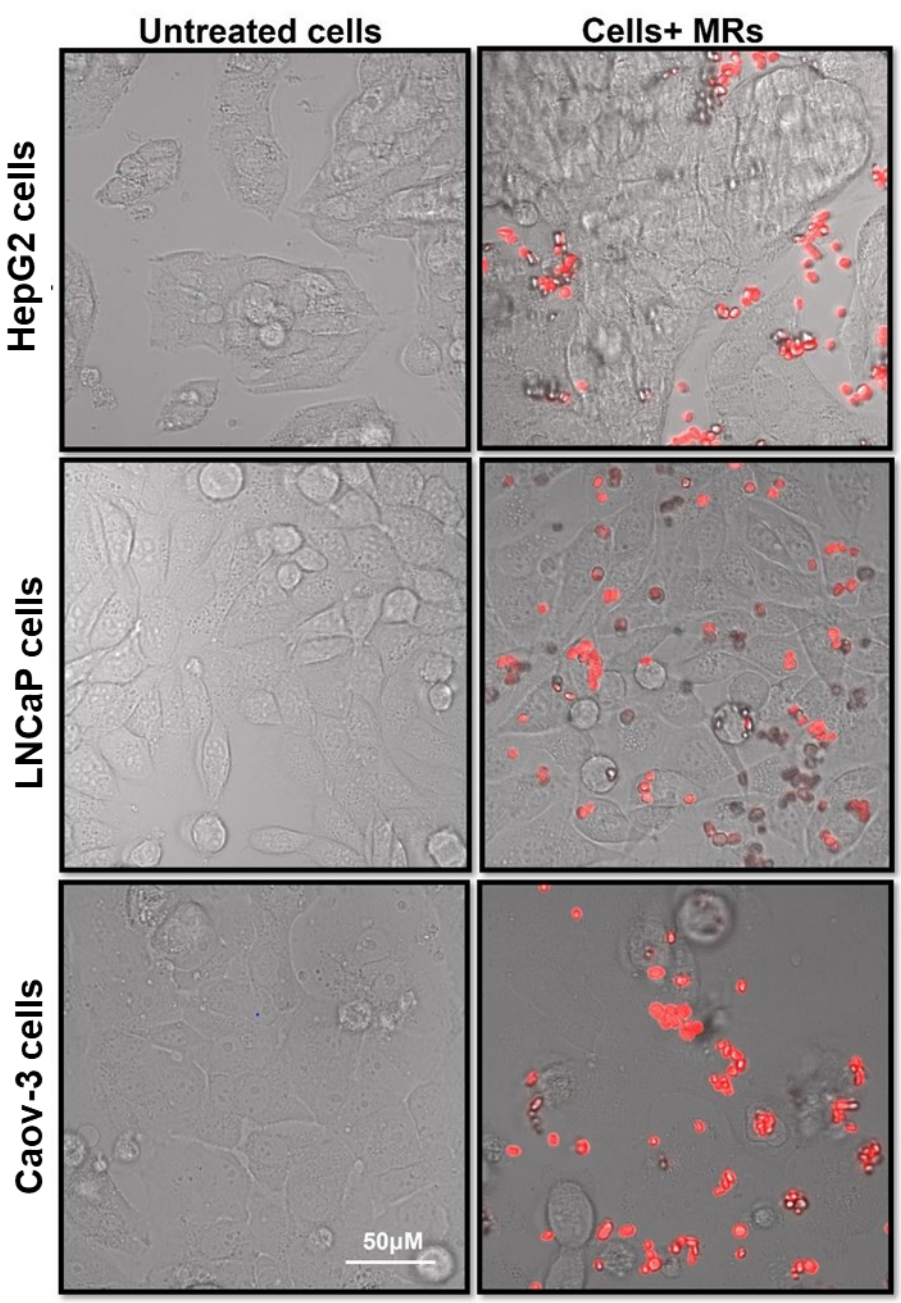

Figure-6: (a) Optical images of cancer cells incubated with DOX-MRs and (b) representative fluorescence images.

The biggest advantage of robotics system is controlled delivery of therapeutic molecules at the target site without any invasive procedure. As we envisaged, cytotoxic concentration of DOX can be controlled by number of MRs being driven towards the cancer cell or tumor site. We collected floating cells and stained with trypan blue to confirm cells with multiple microrobots. However, LNCaP cells were more sensitive to DOX as some dead cells were found with 1-2 MRs (Fig. 7 table). These results suggested that DOX

has higher chemosensitivity in LNCaP cell compared to hepatocarcinoma and ovarian cancer cells. Reports have suggested that HepG2 with wild type p53 (tumor suppressor gene) is least sensitive to DOX when compared with other p53-deleted, and p53-mutated hepatocarcinoma cells.[23] This probably explains the lowered sensitivity of HepG2 cell despites its higher MRs uptake. Time-lapse video also showed changes in cell morphology, and induced cell death within 12 hours assuming DOX release by action of protease enzymes immediately after internalization (Video-2). Taken together, this microrobotic delivery system is a promising candidate for targeted chemotherapy.

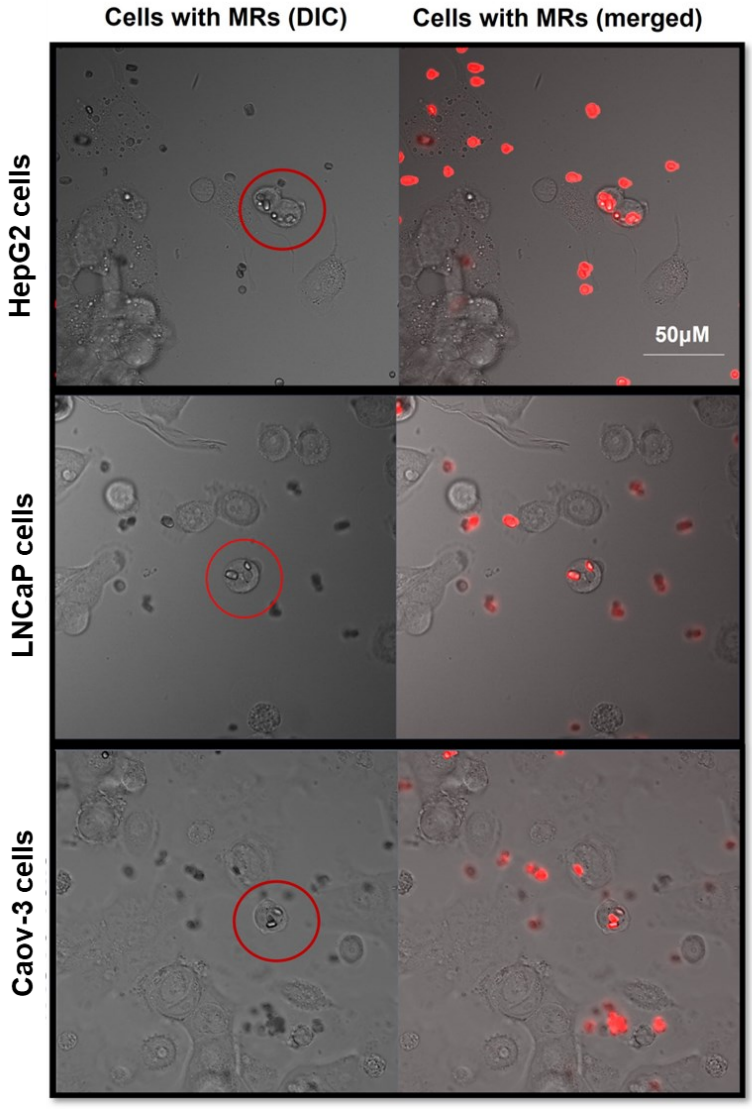

Cell lines	Microrobots/cell
HepG2 cells	**2-3**
LNCaP cells	**1-2**
Caov-3 cells	**2-3**

Figure-7: (a) Assessment of cell death in three cancer cell lines. Dead cells are highlighted in red circles. Cell with multiple number of DOX-MRs were dead showing concentration-dependent cytotoxicity of DOX. (b) Table showing MRs required per single cell to induce DOX-related cytotoxicity.

Conclusion

A simple and effective strategy has been developed to prepare drug-conjugated microrobots. Chemical composition, and surface properties of microrobots are important factors when biocompatibility of drug delivery microrobots are concerned. Moreover, this method can be implemented for conjugation of various biomolecules to microrobots, and controlled delivery of required concentration to the target site which is a prerequisite for various biomedical applications. Nevertheless, a novel magnetic controller design with 3D printed accessories to accommodate the cell petri dish can be useful for various applications (lab-on-a-chip and microfluidic) where real-time monitoring is prerequisite.

References:

1. M. Kuroki, N. Shirasu, *Anticancer Res*. 2014, **34**, 4481-4488.
2. D. T. Debela, S. G. Muzazu, K. D. Heraro, M. T. Ndalama, B. W. Mesele, D. C. Haile, S. K. Kitui, T. Manyazewal, *SAGE open medicine*, 2021, **9**, 20503121211034366.
3. A. Coosemans, A. Vankerckhoven, T , *Eur. J. Cancer*. 2019, 113, 41-44.
4. "The global challenge of cancer." *Nature cancer* 2020, **1**, 1-2.
5. S.W. Smye, A. F. Frangi, *Future Healthc. J*. 2021, **8**, e218-e223.
6. W. Gao, J. Wang, *Nanoscale*. 2014, **6**, 10486-10494.
7. M. Medina-Sánchez. H. Xu, O. G. Schmidt, *Ther. Deliv*. 2018, **9**, 303-316.
8. G. Tezel, S. S. Timur, F. Kuralay, *J. Drug Target*. 2021, **29**, 29-45.
9. R. Wu, Y. Zhu, X. Cai, S. Wu, L. Xu, T. Yu, *Micromachines*. 2022, **13**, 1473.
10. J. Jiang, Z. Yang, A. Ferreira, L. Zhang, *Adv Intell. Syst*. 2022, **4**, 2100279.
11. H. Lee, D. I. Kim, S. H. Kwon, S. Park, *ACS Appl. Mater. Interfaces*. 2021,**13**,19633-19647.
12. A. Terzopoulou, X. Wang, X. Z. Chen, *Adv. Healthc. Mater*. 2020, **9**, e2001031.
13. X. Wang, J. Cai, L. Sun, *ACS Appl. Mater. Interfaces*. 2019, **11**, 4745-4756.
14. H. Lee, H. Choi, M. Lee, S. Park, *Biomed. Microdevices*. 2018, **20**, 103.
15. T. Maric, M. Z. M. Nasir, N. F. Rosli, M. Budanović, R. D. Webster, N. J. Cho, M. Pumera, *Adv Funct Mater.* 2020, **30**, 2000112.
16. X. Song, Z. Chen, X. Zhang, *Sci. Rep*. 2021, **11**, 7907.
17. K. Villa, L. Krejčová, F. Novotný, Z. Heger, Z. Sofer, M. Pumera, *Adv. Funct. Mater.* 2018, **28**, 1804343.
18. K. T. Nguyen, G. Go, Z. Jin, *Adv. Healthc. Mater*. 2021, **10**, 2001681.
19. J Pardo, Z. Peng, R. M. Leblanc, *Molecules*. 2018, **23**, 378.
20. M. Sokolich, D. Rivas, M. Duey, D. Borsykowsky, S. Das, *MethodsX,* 2023, **10**, 102171.
21. S. Bhattacharjee, L. H. de Haan, N. M. Evers, *Part Fibre Toxicol*. 2010, **7**, 25.
22. R. J. Schulze, M. B. Schott, C. A. Casey, P. L. Tuma, M. A. McNiven, *J. Cell Biol*. 2019, **218**, 2096-2112.
23. T. K. Lee, T. C. Lau, I. O. Ng, *Cancer Chemother. Pharmacol*. 2002, **49**, 78-86.

Authors Information

Affiliation: University of Delaware, Newark, Delaware, United States of America, 19716

Sudipta Mallick, Ramadan Abouomar, David Rivas, Max Sokolich, Fatma Ceren Kirmizitas, Aditya Dutta, Sambeeta Das

Contribution:

Sudipta Mallick: Conceptualized and designed the study, executed experiments (cell experiments), wrote the original draft of the manuscript. **Ramadan Abouomar:** Designed the study and executed experiments, **David Rivas**: Performed data analysis, reviewed and edited original draft of the manuscript. **Max Sokolich**: Designed the magnetic controller and executed experiments (Microrobots programing), performed data analysis, wrote original draft of the manuscript. **Fatma Ceren Kirmizitas:** Assisted in biological experiments and edited original draft. **Aditya Dutta**: Supervised biological experiments and edited original draft of the manuscript. **Sambeeta Das**: Conceptualization, Supervised, wrote, and edited original draft of the manuscript.

Acknowledgment

The authors gratefully acknowledge the late Richard West for his help with the cell lines. This project was supported by the Delaware INBRE program, with a grant from the National Institute of General Medical Sciences – NIGMS (P20 GM103446) from the National Institutes of Health and the State of Delaware to SD and AD. This work was also supported by NSF grant OIA2020973 to SD and UDRF-SI grant to AD. This content is solely the responsibility of the authors and does not necessarily represent the official views of NIH.

Data availability Statement

All relevant data are within the paper.

Conflict of Interest

The authors have no conflict of interest to declare.

Supplementary Information

Video-1: Movement of Microrobots being driven towards the cancer cells

Video-2: Time-lapse video of DOX-MRs induced cell death